Published in final edited form as:
Mol Cancer Res. 2009 April ; 7(4): 452–461. doi:10.1158/1541-7786.MCR-08-0451.

Matrix metalloproteinase-activated anthrax lethal toxin inhibits endothelial invasion and neovasculature formation during in vitro morphogenesis

Randall W. Alfano[1,2], **Stephen H. Leppla**[3], **Shihui Liu**[3], **Thomas H. Bugge**[4], **Cynthia J. Meininger**[5], **Terry C. Lairmore**[6], **Arlynn F. Mulne**[7], **Samuel H. Davis**[7], **Nicholas S. Duesbery**[8], and **Arthur E. Frankel**[1,2,*]

1*Cancer Research Institute of Scott & White Memorial Hospital, Temple, TX76502*

2*Department of Internal Medicine, Texas A&M Health Science Center, Temple, TX76502*

3*Laboratory of Bacterial Diseases, National Institute of Allergy and Infectious Diseases, National Institutes of Health, Bethesda, MD20892*

4*Oral and Pharyngeal Cancer Branch, National Institute of Dental and Craniofacial Research, National Institutes of Health, Bethesda, MD20892*

5*Department of Systems Biology and Translational Medicine, Texas A&M Health Science Center, Temple, TX76504*

6*Department of Surgical Oncology, Scott and White Memorial Hospital, Temple, TX76508*

7*Department of Pediatric Hematology/Oncology, Scott and White Memorial Hospital, Temple, TX76508*

8*Laboratory of Cancer and Developmental Cell Biology, Van Andel Research Institute, Grand Rapids, MI 49503*

Abstract

Solid tumor growth is dependent on angiogenesis, the formation of neovasculature from existing vessels. Endothelial activation of the ERK1/2, JNK, and p38 mitogen activated protein kinase (MAPK) pathways is central to this process, and thus presents an attractive target for the development of angiogenesis inhibitors. Anthrax lethal toxin (LeTx) has potent catalytic MAPK inhibition activity. Preclinical studies showed LeTx induced potent tumor growth inhibition via the inhibition of xenograft vascularization. However, LeTx receptors and the essential furin-like activating proteases are expressed in many normal tissues, potentially limiting the specificity of LeTx as an anti-tumor agent. To circumvent nonspecific LeTx activation and simultaneously enhance tumor vascular targeting, a substrate preferably cleaved by the gelatinases class of matrix metalloproteinases (MMPs) was substituted for the furin LeTx activation site. *In vivo* efficacy studies demonstrated that this MMP-activated LeTx inhibited tumor xenografts growth via the reduced migration of endothelial cells into the tumor parenchyma. Here we have expanded on these initial findings by demonstrating that this MMP-activated LeTx reduces endothelial proangiogenic MMP expression, thus causing a diminished proteolytic capacity for extracellular matrix remodeling and endothelial differentiation into capillary networks. Additionally, our data suggests that inhibition of the JNK and p38, but not ERK1/2 pathways is significant in the anti-angiogenic activity of the MMP-activated LeTx.

*Correspondence should be addressed to: Arthur E. Frankel: Cancer Research Institute of Scott and White 5701 South Airport Road Temple, Texas, 76502 E-mail: afrankel@swmail.sw.org.

The authors do not claim a conflict of interest

Collectively, these results support the clinical development of the MMP-activated LeTx for the treatment of solid tumors.

Keywords

anthrax lethal toxin; lethal factor; matrix metalloproteinase; protective antigen; tumor angiogenesis; vascular endothelial growth factor

Introduction

Solid tumor progression is dependent on the tumor's ability to attain nutrients and oxygen via the formation of neovasculature from existing vessels. This process, known as angiogenesis, is triggered by angioproliferative cytokines secreted by oxygen-deprived tumor cells. As a result, endothelial cells of neighboring microvessels are activated causing endothelial proliferation, migration, degradation of surrounding basement membrane, “sprout” invasion into the tumor parenchyma, and eventual formation of tube structures (1,2). Tumor neovascularization fuels continued neoplastic growth, tumor cell dissemination, and eventual formation of distant metastatic colonies that are ultimately responsible for a patient's clinical deterioration (3).

Due to its vital importance in solid tumor growth, angiogenesis has become a subject of intense study in order to identify components of molecular pathways that drive neovasculature formation. Endothelial cell activation of the mitogen activated protein kinase (MAPK) pathways is central to neovessel formation, as individual branches of the MAPK pathway function in different steps of the angiogenic cascade (4,5). Therefore, inhibition of this pathway presents an attractive strategy for tumor-mediated angiogenesis inhibition.

Anthrax lethal toxin (LeTx), secreted from the gram positive *Bacillus anthracis*, is a potent MAPK pathway inhibitor (6). LeTx consists of the 83-kDa Protective Antigen (PA) and the 90-kDa Lethal Factor (LF). Toxin uptake into cells is dependent upon proteolytic activation of PA by ubiquitously expressed furin or furin-like proteases after PA binding to one of two widely expressed receptors, capillary morphogenesis gene 2 (CMG2) and tumor endothelial marker 8 (TEM8) (7). The activated PA subsequently heptamerizes, binds three LF molecules, and migrates into lipid rafts where subsequent internalization occurs. Progressive acidification of endosomal compartments induces PA heptamer pore formation and subsequent LF escape into the cytosol (8). The catalytic activity of LF causes the cleavage and inactivation of the MEKs, with the exception of MEK5, and thus the complete inhibition of the ERK1/2, JNK, and p38 branches of the MAPK pathway (9).

Preclinical studies proved LeTx to be a potent inhibitor of angiogenesis in human tumor xenograft models (9-12). However, PA is quickly processed when injected into the bloodstream due to the expression of the LeTx integrin-like receptors in most tissues in the body and to the presence of various proteases able to cleave the highly basic furin-targeted sequence (13,14). Modification of the furin activation sequence to one preferentially cleaved by enzymes enriched on the surface of angiogenic endothelial cells could potentially circumvent nonspecific PA activation and simultaneously enhance the potency toward the intended target cells. To this end, LeTx was modified by changing the furin cleavage sequence of PA, ^{164}RKKR^{167}, to the sequence ^{164}GPLGMLSQ^{171} that is preferably cleaved by the gelatinase class (MMP-2/-9) of matrix metalloproteinases (MMPs) (15). Gelatinases present an attractive group of PA activating enzymes, since expression of these MMPs has been shown to be upregulated in angiogenic lesions in addition to aiding in cancer progression in a variety of tumor types (16).

This gelatinase-activated PA, designated PA-L1, in combination with LF exhibited impressive anti-tumor efficacy in tumor xenografts in the absence of significant *in vitro* tumor cell cytotoxicity (13). PA-L1/LF-treated xenografts exhibited extensive tumor cell necrosis and a marked absence of CD31 immunostaining (13). Subsequent *in vitro* studies revealed that PA-L1/LF disrupted microvascular endothelial cell migration (13). To expand on these initial findings, and thus better define the anti-angiogenic mechanism, we have examined the effects of LF-mediated MEK cleavage and subsequent endothelial MAPK inhibition on endothelial proliferation, invasion, and tube formation. These results provide further evidence to warrant clinical application of PA-L1/LF.

Results

PA-L1/LF induces only modest cell cycle arrest in microvascular endothelial cells

We measured the [^{3}H] thymidine incorporation to determine whether PA-L1/LF disrupts microvascular endothelial cell proliferation. Treatment with U0126, a MEK1/2 inhibitor, served as a positive control for ERK1/2 inhibition while SP600125 and SB203580 were used for JNK and p38 inhibition, respectively. The wild-type PA in combination with LF was also included for an LF-mediated MAPK inhibition positive control. Each of these compounds effectively inhibited their target MAPK (data not shown but see figure 2). U0126 and SP600125 significantly blocked proliferation by 73 and 94%, respectively. SB203580-mediated p38 inhibition actually induced proliferation in these cells (Fig. 1). By contrast, both 10 nM PA and 10 nM PA-L1 in combination with 5.5 nM LF for 72 hours induced a relatively modest anti-proliferative effect in these cells (Fig. 1 and Supplementary Fig. 1). Thus concentrations of PA-L1/LF that have been observed to induce cell cycle arrest and apoptosis in melanoma cell lines caused only a 35% reduction in endothelial proliferation (17).

To ensure this differential response was not due to inefficient PA-L1 receptor binding/cleavage and LF internalization, we utilized the LF variants FP59 and LF-β-Lac. PA-L1/FP59 was highly cytotoxic to the microvascular endothelial cells, causing a >95% decrease in proliferation (IC_{50} 2 pM) (Fig.1 and Supplementary Fig. 1). Microvascular endothelial cells treated with PA-L1/LF-β-Lac exhibited high levels of intracellular LF-β-Lac activity when compared with cells treated with LF-β-Lac alone, as indicated by the elevated levels of intracellular blue fluorescence (Supplementary Fig. 2). Therefore, these microvascular endothelial cells bind PA-L1 and internalize LF but have modest proliferation inhibition in response to LF-mediated MAPK inhibition.

PA-L1/LF blocks $VEGF_{165}$-mediated microvascular endothelial cell MAPK activation

The evidence above that microvascular endothelial cells internalize LF prompted us to determine whether PA-L1/LF treatment would block endothelial ERK1/2, JNK, and p38 phosphorylation in response to $VEGF_{165}$. Treatment with $VEGF_{165}$ for 45 minutes induced a robust phosphorylation of ERK1/2, which was significantly reduced by 10 nM PA or 10 nM PA-L1 combined with 5.5 nM LF to levels comparable to that of 10 μM U0126-treated cells (Fig. 2A). Densitometric analysis determined an 8-fold decrease in ERK1 phosphorylation and a 25-fold decrease in ERK2 phosphorylation in PA-L1/LF-treated cells (Fig. 2B). Similarly, exposure to 100 ng/ml $VEGF_{165}$ for 20 minutes induced JNK1 (p46) and JNK2 (p54) phosphorylation. Endothelial cell exposure to 10 nM PA/5.5 nM LF and 10 nM PA-L1/5.5 nM LF induced a complete inhibition of JNK1 and JNK2, which was comparable to the small molecule inhibitor SP600125 (Fig. 2C-D). $VEGF_{165}$-mediated activation of the p38 branch was seen after 8 minutes post VEGF addition. Activation of this branch was completely blocked by 10 nM PA/5.5 nM LF and 10 nM PA-L1/5.5 nM LF treatment, as the phosphorylation of this protein was below western blot detection limits (Fig. 2E-F). Thus, PA-L1/LF blocks VEGF165-mediated ERK1/2, JNK and p38 MAPK activation.

The extracellular matrix remodeling potential of microvascular endothelial cells is reduced by PA-L1/LF treatment via the down regulation of proangiogenic MMPs

Since PA-L1/LF blocks MAPK activation in response to proangiogenic cytokines, we subsequently determined whether PA-L1/LF treatment would reduce microvascular endothelial cell invasion through 8 μm diameter pores plugged with extracellular matrix. The invasion of these cells was significantly reduced by >90% after treatment with 10 nM PA-L1/5.5 nM LF ($p < 0.0001$) (Fig. 3A). Additionally, treatment with 20 μM SP600125 or 20 μM SB203580 reduced endothelial invasion by 75 and 48%, respectively (data not shown). ERK1/2 inhibition by 10 μM U0126 had no effect on the invasion of these cells (data not shown).

To better define these initial findings, we employed a fluorescence-based cleavage assay to measure the ability of PA-L1/LF-treated endothelial cells to remodel extracellular matrix. Endothelial cells were treated with 5.5 nM LF alone or in combination with 10 nM PA-L1 and plated onto Matrigel supplemented with 25 μg/ml fluorescein-labeled collagen type I, collagen type IV, or gelatin that is auto-quenched when uncleaved. When cleaved, the extracellular matrix molecule will fluoresce brightly. PA-L1/LF-treated endothelial cells exhibited a significantly reduced ability to cleave these extracellular matrix proteins ($p < 0.0001$) (Fig. 3B). PA-L1/LF treatment reduced the endothelial capacity to cleave collagen type I (Fig 3C) and collagen type IV (Fig. 3D) by 75 and 62%, respectively. Gelatin cleavage was reduced by approximately 30% after PA-L1/LF treatment (Fig. 3E). Endothelial cell adhesion was not affected by PA-L1/LF treatment up to 48 hours (data not shown).

We subsequently measured the effect of PA-L1/LF treatment on expression of four proangiogenic endothelial-derived MMPs that are known to efficiently cleave collagen I, collagen IV, and gelatin. PA or PA-L1 in combination with LF induced a modest and insignificant ~34% increase in MMP-2 expression, as determined by conditioned medium ELISA ($p = 0.1482$) (Fig. 4A) U0126 had a similar effect. By contrast, JNK inhibition by SP600125 and SB203580-mediated p38 inhibition decreased MMP-2 expression by 70 and 64%, respectively (Fig. 4A). Cell lysate gelatin zymography also demonstrated a modest, 2-fold increase in the expression of MMP-2 in PA and PA-L1/LF treated cells as well as U0126-treated cells (Fig. 4B).

In stark contrast however, MMP-1 expression was drastically reduced in 10 nM PA-L1/5.5 nM LF-treated endothelial cells by >99% ($p < 0.0001$) (Fig. 3C). Interestingly, ERK1/2 and JNK activation appears to be important in MMP-1 expression, as U0126 and SP600125 treatment decreased the expression of this MMP by 49 and 62% (Fig. 4C). MMP-10 expression did not seem to be affected by inhibition of any single MAPK branch, but was reduced by 86% by 10 nM PA or 10 nM PA-L1/5.5 nM LF treatment ($p = 0.0086$) (Fig. 4D). The expression of MMP-3, -7, -8, and -13 mRNA was not detected in the untreated endothelial cells (data not shown). Small amounts of MMP-9 mRNA were detected in untreated endothelial cells, but no protein was detected via ELISA (data not shown). MMP-14 transcription was present in untreated endothelial cells but was not affected by PA-L1/LF treatment (data not shown). Therefore, PA-L1/LF treatment induces a significant reduction in MMP-1 and MMP-10 expression.

PA-L1/LF inhibits microvascular endothelial cell tube formation

We subsequently determined how this decrease in endothelial invasive capacity affected the ability of these cells to differentiate into tube structures. Treatment with 10 nM PA or 10 nM PA-L1 in combination with 5.5 nM LF significantly prevented tube formation by 70 and 60% when compared to untreated controls ($p < 0.0001$) (Fig. 5A-B). Closer inspection revealed that endothelial branching that did occur in the PA or PA-L1/LF treated cells appeared to be single

cytoplasmic extensions, whereas branching in untreated controls appeared to be several cells thick (Supplementary Figure 3). Interestingly, U0126 or SP600125 treatments had similar inhibitory effects (Fig. 5A). Treatment with 10μM U0126 or 20μM SP600125 reduced endothelial tube formation by 60 and 50%, respectively. In contrast, however, SB203580 treatment only had a modest and insignificant effect on endothelial cell branching ability. Treatment with 10 nM PA-L1/5.5 nM LF did not affect endothelial cell adhesion (data not shown).

Discussion

Initial preclinical development efforts focused on the application of PA-L1/LF for the treatment of specific subtypes of melanomas, thyroid, and colorectal tumors (18). However, preliminary *in vivo* efficacy studies have suggested the inhibition of angiogenesis, and not direct tumor cell cytotoxicity, as the primary anti-tumor mechanism (13). We have expanded on these initial findings by demonstrating that PA-L1/LF treatment blocks VEGF-induced endothelial MAPK activation, leading to a reduction in the endothelial invasive capability. These findings account for the poor vascularization of Matrigel plugs *in vivo* and in part explain how LF decreases microvascular density of tumors *in vivo* (9,10,12,13). Further, we have provided evidence that the anti-angiogenic activity of PA-L1/LF resembles that of JNK and p38, but not ERK1/2, MAPK branch inhibition.

The current study indicates that *in vitro* PA-L1/LF action is independent of endothelial cell cytotoxicity. Selective inhibition of ERK1/2 and JNK branches has previously been shown to induce endothelial cell cycle arrest (19,20). However, inhibition of p38 has been shown to enhance endothelial proliferation (21). This study suggests that the anti-proliferative effects of ERK1/2 and JNK inhibition are counterbalanced by the pro-proliferative effect of p38 inhibition. Thus, the net effect is modest anti-proliferative effect of the pan-MAPK inhibitor PA-L1/LF.

Although proliferation was by comparison only modestly affected, PA-L1/LF significantly reduced endothelial proteolytic capacity to cleave collagen type I, collagen type IV, and gelatin. Endothelial-derived proangiogenic MMPs that are known to cleave these substrates include MMP-1, -2, -9, and -10 (22). Our studies indicated that PA-L1/LF treatment induced a dramatic reduction in MMP-1 and -10. However, we cannot rule out the contribution of other extracellular matrix remodeling enzymes that may be affected by PA-L1/LF treatment. It has been shown that the expression of the cysteine protease cathepsin L was reduced in LeTx-treated V12 H-ras-transformed cells (9). Taken together, it can be speculated that the cumulative effects of this decrease in endothelial cell proteolytic potential combined with the reduced migration of these cells translated to the failure tumor vascularization *in vivo* (13).

Attempts to dissect the roles of each MAPK pathway revealed that the anti-angiogenic effects of PA-L1/LF resemble that of JNK and p38 MAPK pathway inhibition. Selective inhibition of JNK by SP600125 or p38 by SB203580 has been shown to significantly inhibit endothelial cell migration *in vitro* in the absence of endothelial cell cytotoxicity (23,24,25). Similarly, endothelial extracellular matrix remodeling enzyme expression is dependent on the activation of c-Jun, downstream of JNK. Our data are in agreement with these studies in that selective JNK and p38 inhibition both by pathway-specific inhibitors and by the pan-inhibitor PA-L1/LF significantly reduced the invasion of microvascular endothelial cells *in vitro*.

The contribution of the ERK1/2 pathway in PA-L1/LF-mediated angiogenesis inhibition is less clear. Although our studies indicated that ERK1/2 inhibition via U0126 reduced endothelial cell proliferation and significantly altered *in vitro* tube formation capacity, we found that selective ERK1/2 inhibition had no effect on endothelial cell invasion. Despite this,

another group has shown that *in vivo* transfection of a dominant-negative MEK1 into endothelial cells suppresses angiogenesis and tumor growth (26). Collectively, these results indicate while the primary role of ERK1/2 signaling *in vitro* is to regulate cell proliferation, this signaling pathway may play additional roles in endothelial function *in vivo* (27).

Other studies have shown that PA-L1/LF mediated MAPK inhibition reduces tumor cell proangiogenic cytokine expression (13). Thus, it can be speculated that PA-L1/LF may have a dual anti-angiogenesis mechanism in which tumor cell cytokine expression is reduced as well as endothelial invasive and migratory potential. However, we previously observed that conditioned medium from PA-L1/LF-treated tumor cells retain the ability to attract endothelial cells *in vitro*. Further, conditioned medium from PA-L1/LF treated tumor cells activate endothelial ERK1/2 as efficiently as untreated controls. Therefore, this observed decrease in tumor cell angioproliferative cytokines cannot be considered as a primary mechanism for the failure of neovasculature formation *in vivo* but may have relevance in tumor models with preexisting vasculature (13). Ding et al. demonstrated a rapid (>24 h) decrease in the perfusion of well vascularized fibrosarcoma xenografts with a single dose of LeTx, leading to a decrease in tumor growth (12). It is possible that this LF-mediated reduction in tumor cell VEGF expression induces a decrease in endothelial NO production, thus causing a vasoconstriction and reduced tumor perfusion (12,28). Combined with a reduction in endothelial extracellular matrix binding, tumor microvascular function could be severely compromised (12).

Taken together, these results indicate that the explicit targeting of endothelial MAPK activation appears to be a viable approach for angiogenesis inhibition. Similar findings have been presented with other MAPK inhibitors. BAY 43-9006 (Sorafenib) is a bi-aryl urea compound that inhibits both c-RAf and B-Raf kinases (29). BAY 43-9006 has been shown to significantly hinder tumor growth in xenograft models of several human tumors without significant tumor cell cytotoxicity *in vitro* (30). BAY 43-9006-treated tumors exhibit a marked reduction in neovascularization, as determined by CD31 immunohistochemistry, with massive tumor necrosis detected (30). Similarly, the MEK inhibitor CI-1040 significantly hindered the vascularization of Matrigel plugs *in vivo* (31).

In conclusion, the catalytic MAPK inhibition activity demonstrated by PA-L1/LF translates to potent anti-angiogenic effects via the decreased endothelial invasive capacity. These observations in part explain the impressive anti-tumor activity observed *in vivo* with PA-L1/LF treatment. Further, these findings warrant the further clinical development of this modified anthrax toxin. The explicit targeting of angiogenic endothelial cells will potentially translate to clinical versatility, as any solid tumor patient would respond to systemic PA-L1/LF therapy.

Materials and Methods

Reagents

PA, PA-L1, LF, FP59, and LF-β-Lac were produced as previously described (15,32,33). The fusion protein LF-β-Lac consists of the PA binding domain of LF genetically fused to *E. coli* β-lactamase (32). FP59 consists of the first 254 amino acids of LF (the PA/PA-L1 binding domain) fused to the catalytic portion of *Pseudomonas* exotoxin A (amino acids 362-613) (33). FP59, when internalized in a PA/PA-L1-dependent mechanism inhibits protein synthesis and thus is toxic to all cells (33). The MEK1/2 inhibitor U0126 ethanolate, the JNK inhibitor SP600125, the p38 MAPK inhibitor SB203580, were purchased from Sigma-Aldrich (St. Louis, MO).

Cell Culture

Adult dermal microvascular endothelial cells (HMVEC-dAd) were purchased from Lonza (Basel, Switzerland) and cultured on flasks coated with 1.5% bovine type B gelatin (Sigma Alrich) prepared with Dulbecco's phosphate buffered saline (Invitrogen, Carlsbad, CA) in complete endothelial cell medium (EGM supplemented with bovine brain extract, hEGF, hydrocortisone, GA-1000 (Gentamicin, Amphotericin B), and 5% fetal bovine serum) (Lonza). Endothelial cells were maintained at 37°C in a 5% CO_2 environment. All experiments were conducted on cells between passages 4 and 8.

Cytotoxicity Assay

The ^{3}H-thymidine incorporation inhibition assay was utilized as described previously (17). Cells were resuspended in complete growth medium at a density of 8×10^5 cells/ml. One hundred μl were plated per well in Costar 96-well flat-bottomed plates. Cells were allowed to recover overnight, and the medium was exchanged for complete growth medium with or without 5.5 nM LF/1.9 nM FP59 at final concentration. Serially diluted PA/PA-L1 at final concentrations of 0-10,000 pM or small molecule inhibitors U0126, SP600125, and SB203580 ranging from a final concentration of 0-60,000 nM were added. After 48 hours at 37°C/5% CO_2, one microcurie of ^{3}H-thymidine (NEN DuPont, Boston, MA) in 50 μL of complete medium per well was added and incubated at 37°C/5% CO_2 for an additional 18 hours. The cells were then harvested with a Skatron Cell Harvester (Skatron Instruments, Lier, Norway) onto glass fiber mats, and counts per minute (CPM) of incorporated ^{3}H-thymidine were quantified using an LKB liquid scintillation counter (Perkin Elmer, Waltham, MA). The concentration of toxin that inhibited ^{3}H-thymidine incorporation by 50% compared to control wells was defined the IC_{50}. The percent maximal ^{3}H-thymidine incorporation was plotted versus the log of the toxin concentrations, and nonlinear regression with a variable slope sigmoidal dose-response curve was generated along with IC_{50} using GraphPad Prism software (GraphPad Software). Assays were performed in triplicate with IC_{50} variability between assays less than 30%.

Western Blot

One hundred thousand HMVEC-dAd cells were grown to confluence on 1.5% gelatin coated 60mm dishes (Fisher Scientific, Pittsburgh, PA). Cells were pretreated with DMSO vehicle, 10 μM U0126, 20 μM SP600125, 20 μM SB203580, 5.5 nM LF alone or in combination with 10 nM PA/PA-L1 for eight h in complete growth medium. Cells were then serum starved for 16 h in the presence of the toxins/inhibitors and then stimulated with 100ng/ml $VEGF_{165}$ (R&D Systems, Minneapolis, MN) for time intervals specific for maximal phosphorylation of each MAPK pathway branch as previously determined. Cells were washed once with ice-cold DPBS and immediately lysed in lysis buffer (25 mM Hepes, pH 7.6, 0.3 M NaCl, 1.5 mM $MgCl_2$ 0.2 mM EDTA, 0.1% Triton X-100, 0.5 mM DTT, 0.1 mM sodium orthovanadate, 1 mM PMSF) with protease inhibitor cocktail (Sigma-Aldrich). Lysates were solubilized on ice for 30 min and spun for 20 min at 15000xg. Equal amounts of lysates were separated on an 8-16% Tris-Glycine gels (Invitrogen) and transferred to a nitrocellulose membrane. Membranes were blocked with 5% w/v milk, 1X TBS for 1 h at room temperature and then probed with rabbit anti phospho-p54/p46 SAPK/JNK (Thr183/Tyr185), phospho-p38 MAPK (Thr180/Tyr182), or phospho-ERK1/2 (Thr202, Tyr204) (Cell Signaling Technology, Danvers, MA) in 5% w/v BSA, 1X TBS, .1% Tween-20 at 4°C overnight. Blots were then washed and treated with peroxidase-conjugated goat anti-rabbit secondary antibodies (Jackson Immunoresearch, West Grove, PA) for 1 hour, washed, and developed via LumiGLO chemiluminescence reagent (Cell Signaling Technology). Blots were subsequently probed with appropriate antibodies to determine total amounts of the proteins (Cell Signaling Technology), and developed as described above. Membranes were then stripped, probed for actin (Sigma-Aldrich), and

developed to ensure equal loading. Band intensity was determined by the Fluorchem SP densitometer (Alpha Innotech, San Leandro, CA) and data are presented as a percent of the 100ng/ml VEGF control.

Endothelial Invasion

The CytoSelect™ 96-well invasion kit (Cell Biolabs, San Diego, CA) was utilized to determine invasive potential after PA-L1/LF treatment. Confluent monolayers of cells in 6-well plates were pretreated with 5.5 nM LF alone or in combination with 10 nM PA-L1 for 24 h, trypsinized, and resuspended in serum-free medium containing the toxins at a density of 5×10^5 cells/ml. Basal medium or medium containing 20% FBS was placed in the bottom chambers and 100 μl of the cell suspensions were loaded per upper chamber. Cells were allowed to invade for 24 h at 37°C/5%CO_2. Cells that had invaded to the other side of the inserts were harvested and counted. Data are expressed as a percent of the untreated controls.

MMP ELISA

One hundred thousand HMVEC-dAd cells were plated per well in uncoated 12-well plates and allowed to adhere overnight. Cells were then treated with specified concentrations of toxins/inhibitors in complete growth medium for 12 h. Medium was then exchanged for basal medium containing the toxins/inhibitors and cells were serum starved for 16 h. Cells were then stimulated with complete growth medium supplemented with 100 ng/ml $VEGF_{165}$ in the presence of the toxins/inhibitors for 48 h. Conditioned medium was collected and spun at 15000xg for 30 min to remove cell debris, and medium was assayed for total MMP-1 (Raybio, Norcross GA), MMP-2, MMP-9, and MMP-10 (R&D Systems) following the manufacturer's instructions.

Gelatin Zymography

Cell lysate gelatin zymography was performed as described previously (17). HMVEC-dAd cells were grown to confluence in 6-well plates. Cells were serum starved for 16 h in the presence of the toxins/inhibitors. Medium was then exchanged for complete growth medium supplemented with 100 ng/ml $VEGF_{165}$ (R&D Systems) in the presence of the toxins/inhibitors and cells were incubated at 37°C/5%CO_2 for 48 h. The medium was removed and the cells were washed with DPBS twice. Cells were lysed on ice for 10 min using 0.5 ml lysis buffer per well (0.5% (V/V) Triton X-100 in 0.1 M Tris-HCl, pH 8.1), and removed with a rubber scrapper. Lysates were spun at 15,000xg using an Allegra 2502 centrifuge fitted with TA-10-250 rotor (Beckman Coulter, Fullerton, CA). Cell lysate protein concentration determined using the BCA procedure (Pierce, Rockford, IL) and adjusted to .65 mg/ml with lysis buffer. The lysate fraction contained plasma membrane sheets and vesicles, so that MMP-2 activities in the cell lysate were considered as cell surface gelatinase activities. For concentration of gelatinases, 80 μg cell lysate protein was incubated with 50 μl gelatin Sepharose beads (GE, St. Giles, UK) in equilibration buffer (50 mM Tris-HCl, 150 mM NaCl, 5 mM $CaCl_2$, 0.02% (V/V) Tween-20, 10 mM EDTA, pH 7.6) for 1 h at 4°C on an end-over-end mixer. Cell lysates were spun at 500xg for 10 min at 4°C using a Microfuge 18 centrifuge (Beckman Coulter) and resuspended in 500 μl Wash Buffer (50 mM Tris-HCl, 200 mM NaCl, 5 mM $CaCl_2$, 0.02% (V/V) Tween-20, 10 mM EDTA, pH 7.6). After 4 washes with Wash Buffer, beads were resuspended in 30 μl 2X Tris-Glycine sample buffer (Invitrogen), and loaded in 10% gelatin zymogram gels (Invitrogen). Gels were run at 125 mV for 90 min, and developed according to Invitrogen. The recombinant 68-kD pro-form of MMP-2 (Millipore, Billerica, MA) served as a positive control for MMP-2 activity.

Fluorescent Extracellular Matrix Cleavage

HMVEC-dAd cells were grown to confluence in 6 well plates and pretreated with the specified concentrations of toxins/inhibitors for 48 hours. Prior to the start of the experiment, 8-well chamber slides (Lab-tek, Rochester, NY) were coated with 150μl Matrigel™ supplemented with 25μg/ml dye-quenched (DQ) fluorogenic gelatin, collagen I, or collagen IV (Invitrogen) and was allowed gel for 1 hour at 37°C/5% CO_2. Cells were trypsinized and resuspended in serum-free medium with or without the toxins/inhibitors at a density of 5×10^5 cells/ml. One hundred μl of the cell suspension was added per well and cells were incubated at 37°C/5% CO_2 for 7 hours. The extent of DQ gelatin, collagen I, collagen IV cleavage was visualized via an IX-71 inverted microscope fitted with a FluoView 300 confocal scanning head with FluoView version 5.0 software (Olympus Center Valley, PA). Three areas of each chamber were randomly selected per experiment and images were obtained by variable thickness of scans for 15 scans keeping laser intensity and PMT constant. Images were analyzed for activated green pixels in a fixed area of 5 random areas of each image and data is presented as a percent of green fluorescence in the drug-free controls.

Endothelial Tube Formation Inhibition

HMVEC-dAd cells were grown to confluence in 6-well plates. Cells were pretreated with specified concentrations of toxins/inhibitors for 18 h. Cells were then trypsinized, and resuspended at a concentration of 50,000 cells/ml in serum-free medium containing the toxins/inhibitors. Fifty thousand cells were plated in 8-well chamber slides (Lab-Tek) coated with 150 μl Matrigel™. Cells were allowed to undergo tube formation for 7 h at 37°C/5% CO_2 and then stained with 1X Calcein AM (Cell Biolabs) according to the manufacturer's instructions. Tube structures were visualized via an IX-71 inverted microscope fitted with a FluoView 300 confocal scanning head with FluoView version 5.0 software. Five areas of each chamber were randomly selected per experiment and images were obtained by variable thickness of scans for 15 scans keeping laser intensity and PMT constant. Images were analyzed for branching endothelial connections and data was analyzed as the percent of branching connections in the drug-free controls.

Statistical Analysis

Significance of correlations was performed using GraphPad Prism software (GraphPad Software). Unpaired t-tests were used for all analyses assuming Gaussian populations with a 95% confidence interval.

Supplementary Material

Refer to Web version on PubMed Central for supplementary material.

Acknowledgements

We thank Drs. Shu-Ru Kuo, Yunpeng Su, and Jung Woo for helpful discussions and critical reading of the manuscript, as well as Anna Webb and the Texas A&M Imagining Facility for technical assistance and Rasem Fattah for assistance with protein purification. This research was supported by the Intramural Research Program of the NIH, National Institute of Allergy and Infectious Diseases.

This work was supported by the Departments of Surgery and Pediatric Hematology/Oncology of Scott & White Memorial Hospital

Abbreviations

PA, protective antigen; LF, lethal factor; LeTx, anthrax lethal toxin; MMP, matrix metalloproteinase; VEGF, vascular endothelial growth factor.

References

1. Izawa JI, Dinney CP. The role of angiogenesis in prostate and other urologic cancers: a review. CMAJ 2001;164:662–70. [PubMed: 11258215]
2. Van den Beucken T, Kortizinsky M, Wouters BG. Translational control of gene expression during hypoxia. Cancer Biol Ther 2006;5:749–55. [PubMed: 16861930]
3. Folkman J. Angiogenesis in cancer, vascular, rheumatoid and other disease. Nat Med 1995;1:27–31. [PubMed: 7584949]
4. Depeille PE, Bromberg-White JL, Duesbery NS. MKK signaling and vascularization. Oncogene 2007;26:1290–6. [PubMed: 17322914]
5. Murphy DA, Makonnen S, Lassoued W, Feldman MD, Carter C, Lee WM. Inhibition of tumor endothelial ERK activation, angiogenesis, and tumor growth by sorafenib (BAY43-9006). Am J Pathol 2006;169:1875–85. [PubMed: 17071608]
6. Duesbery NS, Webb CP, Leppla SH, Gordon VM, Klimpel KR, Copeland TD, et al. Proteolytic inactivation of MAP-kinase-kinase by anthrax lethal factor. Science 1998;280:734–7. [PubMed: 9563949]
7. Young JA, Collier RJ. Anthrax toxin: receptor binding, internalization, pore formation, and translocation. Annu Rev Biochem 2007;76:243–65. [PubMed: 17335404]
8. Puhar A, Montecucco C. Where and how do anthrax toxins exit endosomes to intoxicate host cells? Trends Microbiol 2007;15:477–82. [PubMed: 17983750]
9. Duesbery NS, Resau J, Webb CP, Koochekpour S, Koo HM, Leppla SH, et al. Suppression of ras-mediated transformation and inhibition of tumor growth and angiogenesis by anthrax lethal factor, a proteolytic inhibitor of multiple MEK pathways. Proc Natl Acad Sci USA 2001;98:4089–94. [PubMed: 11259649]
10. Depeille P, Young JJ, Boquslawski EA, Berghuis BD, Kort EJ, Resau JH, et al. Anthrax lethal toxin inhibits growth of and vascular endothelial growth factor release from endothelial cells expressing the human herpes virus 8 viral G protein coupled receptor. Clin Cancer Res 2007;13:5926–34. [PubMed: 17908989]
11. Huang D, Ding Y, Lou WM, Bender S, Qian CN, Kort E, et al. Inhibition of MAPK kinase signaling pathways suppressed renal cell carcinoma growth and angiogenesis in vivo. Cancer Res 2008;68:81–8. [PubMed: 18172299]
12. Ding Y, Boguslawski EA, Berghuis BD, Young JJ, Zhang Z, Hardy K, et al. Mitogen-activated protein kinase kinase signaling promotes growth and vascularization of fibrosarcoma. Mol Cancer Ther 2008;7:648–58. [PubMed: 18319331]
13. Liu S, Wang H, Currie BM, Molinolo A, Leung HJ, Moayeri M, et al. Matrix metalloproteinase-activated anthrax lethal toxin demonstrates high potency in targeting tumor vasculature. J Biol Chem 2007;283:529–40. [PubMed: 17974567]
14. Moayeri M, Wiggins JF, Leppla SH. Anthrax protective antigen cleavage and clearance from the blood of mice and rats. Infect Immun 2007;75:5175–84. [PubMed: 17724066]
15. Liu S, Netzel-Arnett S, Birkedal-Hansen H, Leppla SH. Tumor cell-selective cytotoxicity of matrix metalloproteinase-activated anthrax toxin. Cancer Res 2000;60:6061–7. [PubMed: 11085528]
16. Turpeenniemi-Hujanen T. Gelatinases (MMP-2 and -9) and their natural inhibitors as prognostic indicators in solid cancers. Biochimie 2005;87:287–97. [PubMed: 15781315]
17. Alfano RW, Leppla SH, Liu S, Bugge TH, Herlyn M, Smalley KS, et al. Cytotoxicity of the matrix metalloproteinase-activated anthrax lethal toxin is dependent on gelatinase expression and B-RAF status in human melanoma cells. Mol Cancer Ther 2008;7:1218–26. [PubMed: 18483309]
18. Alfano RW, Leppla SH, Liu S, Bugge TH, Duesbery NS, Frankel AE. Potent inhibition of tumor angiogenesis by the matrix metalloproteinase-activated anthrax lethal toxin: implications for broad anti-tumor efficacy. Cell Cycle Mar 15;2008 7(6):745–9. [PubMed: 18245947]
19. Shu X, Wu W, Mosteller RD, Broek D. Sphingosine kinase mediates vascular endothelial growth factor-induced activation of ras and mitogen-activated protein kinases. Mol Cell Biol 2002;22:7758–68. [PubMed: 12391145]
20. Meadows KN, Bryant P, Pumiglia K. Vascular endothelial growth factor induction of the angiogenic phenotype requires Ras activation. J Biol Chem 2001;276:49289–98. [PubMed: 11682481]

21. Yu Y, Sato JD. MAP kinases, phosphatidylinositol 3-kinase, and p70 S6 kinase mediate the mitogenic response of human endothelial cells to vascular endothelial growth factor. J Cell Physiol 1999;178:235–46. [PubMed: 10048588]
22. Noël A, Jost M, Maquoi E. Matrix metalloproteinases at cancer tumor-host interface. Semin Cell Dev Biol 2008;19:52–60. [PubMed: 17625931]
23. Wu J, Yan H, Chen W, Chen W, Wang C, Chi Y, et al. JNK signaling pathway is required for bFGF-mediated surface cadherin downregulation on HUVEC. Exp Cell Res 2007;314:421–9. [PubMed: 18164704]
24. Rousseau S, Houle F, Landry J, Huot J. p38 MAP kinase activation by vascular endothelial growth factor mediates actin reorganization and cell migration in human endothelial cells. Oncogene 1997;15:2169–77. [PubMed: 9393975]
25. Ennis BW, Fultz KE, Smith KA, Westwick JK, Zhu D, Boluro-Ajayi M, et al. Inhibition of tumor growth, angiogenesis, and tumor cell proliferation by a small molecule inhibitor of c-Jun N-terminal kinase. J Pharmacol Exp Ther 2005;313:325–32. [PubMed: 15626722]
26. Mavria G, Vercoulen Y, Yeo M, Paterson H, Karasarides M, Marais R, et al. ERK-MAPK signaling opposes Rho-kinase to promote endothelial cell survival and sprouting during angiogenesis. Cancer Cell 2006;9:33–44. [PubMed: 16413470]
27. Yang B, Cao DJ, Sainz I, Colman RW, Guo YL. Different roles of ERK and p38 MAP kinases during tube formation from endothelial cells cultured in 3-dimensional collagen matrices. J Cell Physiol 2004;200:360–9. [PubMed: 15254963]
28. Horowitz JR, Rivard A, van der Zee R, Hariawala M, Sheriff DD, Esakof DD, et al. Vascular endothelial growth factor/vascular permeability factor produces nitric oxide-dependent hypotension. Evidence for a maintenance role in quiescent adult endothelium. Arterioscler Thromb Vasc Biol 1997;17:2793–800. [PubMed: 9409257]
29. Awada A, Hendlisz A, Gil T, Bartholomeus S, Mano M, de Valeriola D, et al. Phase I safety and pharmacokinetics of BAY 43-9006 administered for 21 days on/7 days off in patients with advanced, refractory solid tumours. Br J Cancer 2005;92:1855–61. [PubMed: 15870716]
30. Wilhelm SM, Carter C, Tang L, Wilkie D, NcNabola A, Rong H, et al. BAY 43-9006 exhibits broad spectrum oral antitumor activity and targets the RAF/MEK/ERK pathway and receptor tyrosine kinases involved in tumor progression and angiogenesis. Cancer Res 2004;64:7099–109. [PubMed: 15466206]
31. McDaid HM, Lopez-Barcons L, Grossman A, Lia M, Keller S, Pérez-Soler R, et al. Enhancement of the therapeutic efficacy of taxol by the mitogen-activated protein kinase kinase inhibitor CI-1040 in nude mice bearing human heterotransplants. Cancer Res 2005;65:2854–60. [PubMed: 15805287]
32. Hobson JP, Liu S, Rono B, Leppla SH, Bugge TH. Imaging specific cell-surface proteolytic activity in single living cells. Nat Methods 2006;3:259–61. [PubMed: 16554829]
33. Arora N, Klimpel K, Singh Y, Leppla S. Fusions of anthrax toxin lethal factor to the ADP-ribosylation domain of Pseudomonas exotoxin A are potent cytotoxins which are translocated to the cytosol of mammalian cells. J Biol Chem 1992;267:15542–8. [PubMed: 1639793]

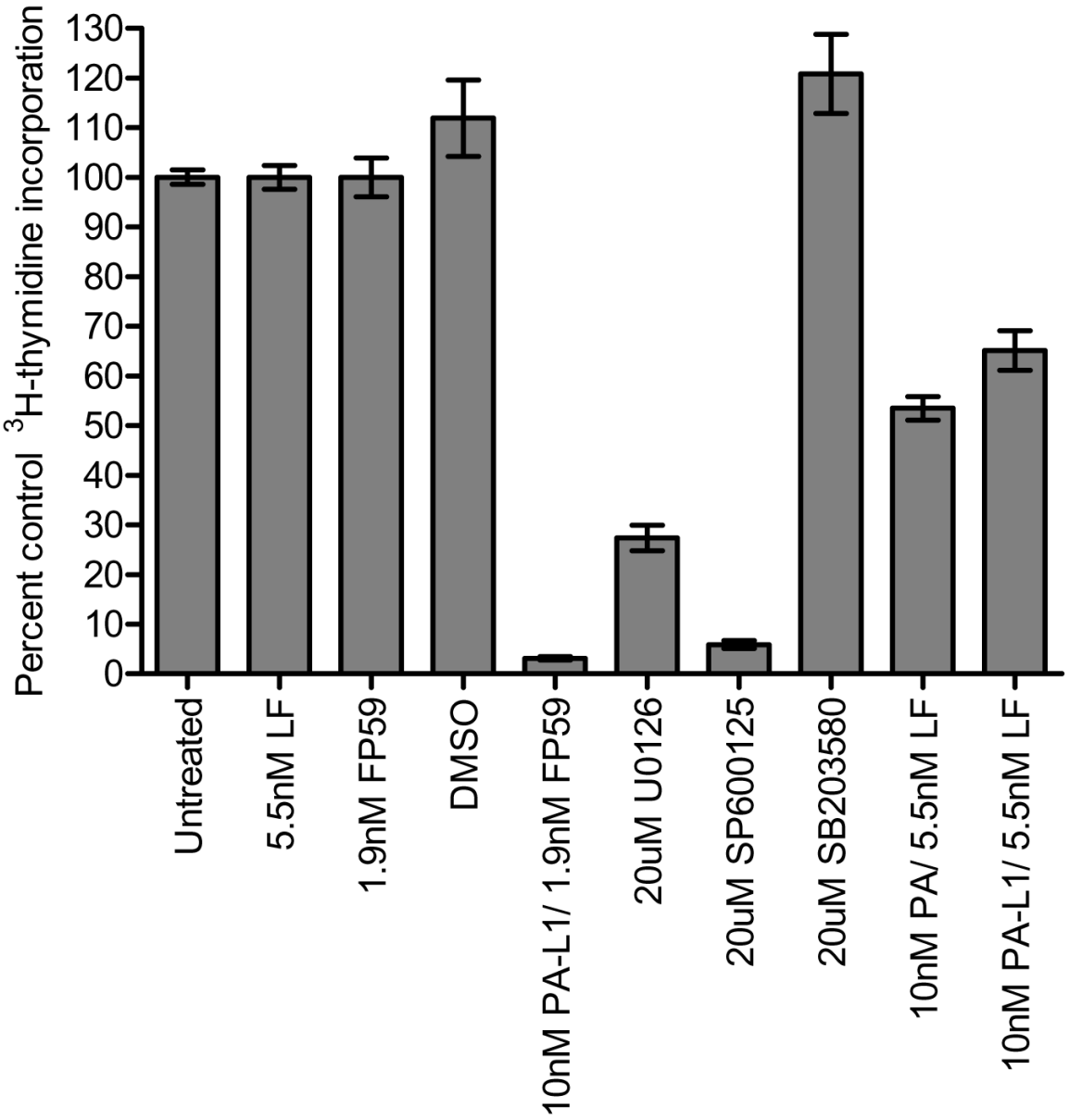

Figure 1.

PA-L1/LF has modest anti-proliferative effects on microvascular endothelial cells. Human microvascular endothelial cells were treated with small molecule inhibitors or toxins and the incorporation of ^{3}H-thymidine was measured. Data is expressed as a percent of the untreated cells ^{3}H-thymidine incorporation. 10 nM PA and 10 nM PAL1/5.5 nM LF induced only a 47 and 35% proliferation inhibition, respectively, when compared to the untreated and 5.5 nM LF/1.9 nM FP59 controls (IC_{50} >10,000 pmol/L). As expected, treatment with the MEK1/2 inhibitor U0126 (20 μM) as well as the JNK inhibitor SP600125 (20 μM) significantly blocked endothelial proliferation by 73 and 94% (IC_{50} 4 μmol/L and 1.8 μmol/L for U0126 and SP600125, respectively). 20μM SB203580-mediated p38 inhibition actually induced proliferation in these cells. Endothelial cells were sensitive to 10nM PA-L1/1.9nM FP59 (IC_{50} 2 pmol/L), reducing proliferation by >95%. FP59 consists of the first 254 amino acids of LF (the PA/PA-L1 binding domain) fused to the catalytic portion of *Pseudomonas* exotoxin

A (amino acids 362-613). When internalized in a PA/PA-L1 dependent mechanism, FP59 inhibits protein synthesis and thus is toxic to all cells.

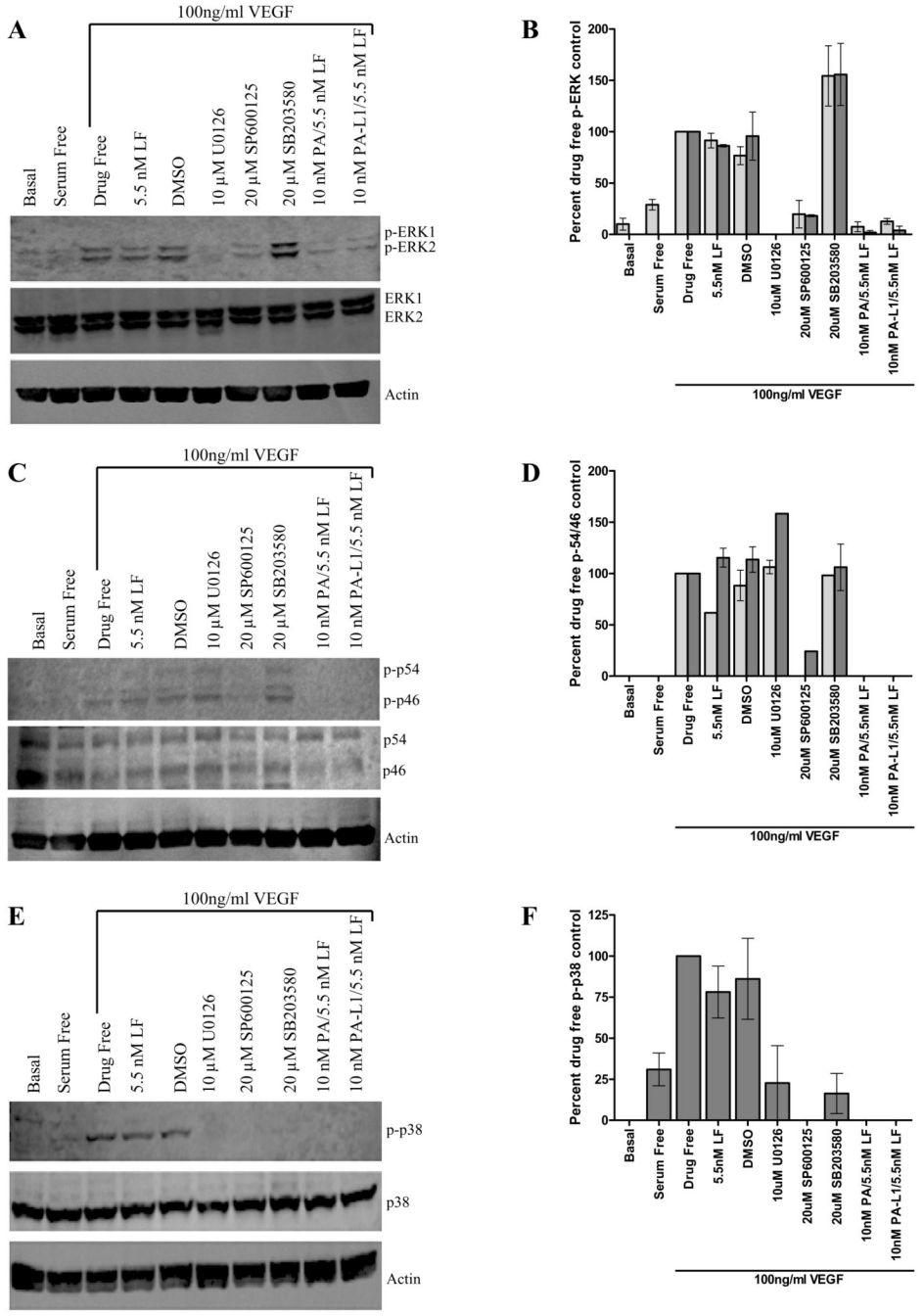

Figure 2.

PA-L1/LF blocks $VEGF_{165}$-mediated microvascular endothelial cell MAPK activation. Pretreated serum starved endothelial cells were exposed to 100 ng/ml $VEGF_{165}$ for 45, 20, or 8 minutes in order to determine ERK1/2, JNK, and p38 activation levels, respectively. Data is expressed as a percent of the phosphorylated protein in the 100ng/ml VEGF positive controls. (A) 10 nM PA and 10 nM PA-L1 in combination with 5.5 nM LF blocked $VEGF_{165}$-mediated ERK1/2 phosphorylation comparable to the inhibition observed by 10 μM U0126. (B) Densitometric analysis determined a ~8-fold difference between the PA-L1/LF treated and 100 ng/ml VEGF positive controls in ERK1 (light gray bars) phosphorylation and a ~25-fold difference in ERK2 (dark gray bars) phosphorylation levels. U0126 treated endothelial cells

exhibited phosphorylation levels below western detection limits (C) 10 nM PA and 10 nM PA-L1/5.5 nM LF induced a complete inhibition of JNK1 (p46) (light gray bars) and JNK2 (p54) (dark gray bars) phosphorylation, which was comparable to the small molecule inhibitor SP600125 (D). (E) $VEGF_{165}$-mediated activation of the p38 branch was also completely blocked by 10 nM PA/5.5 nM LF and 10 nM PA-L1/5.5 nM LF treatment. (F) Densitometric analysis determined p38 phosphorylation not significant from background in PA and PAL1/LF treated cells.

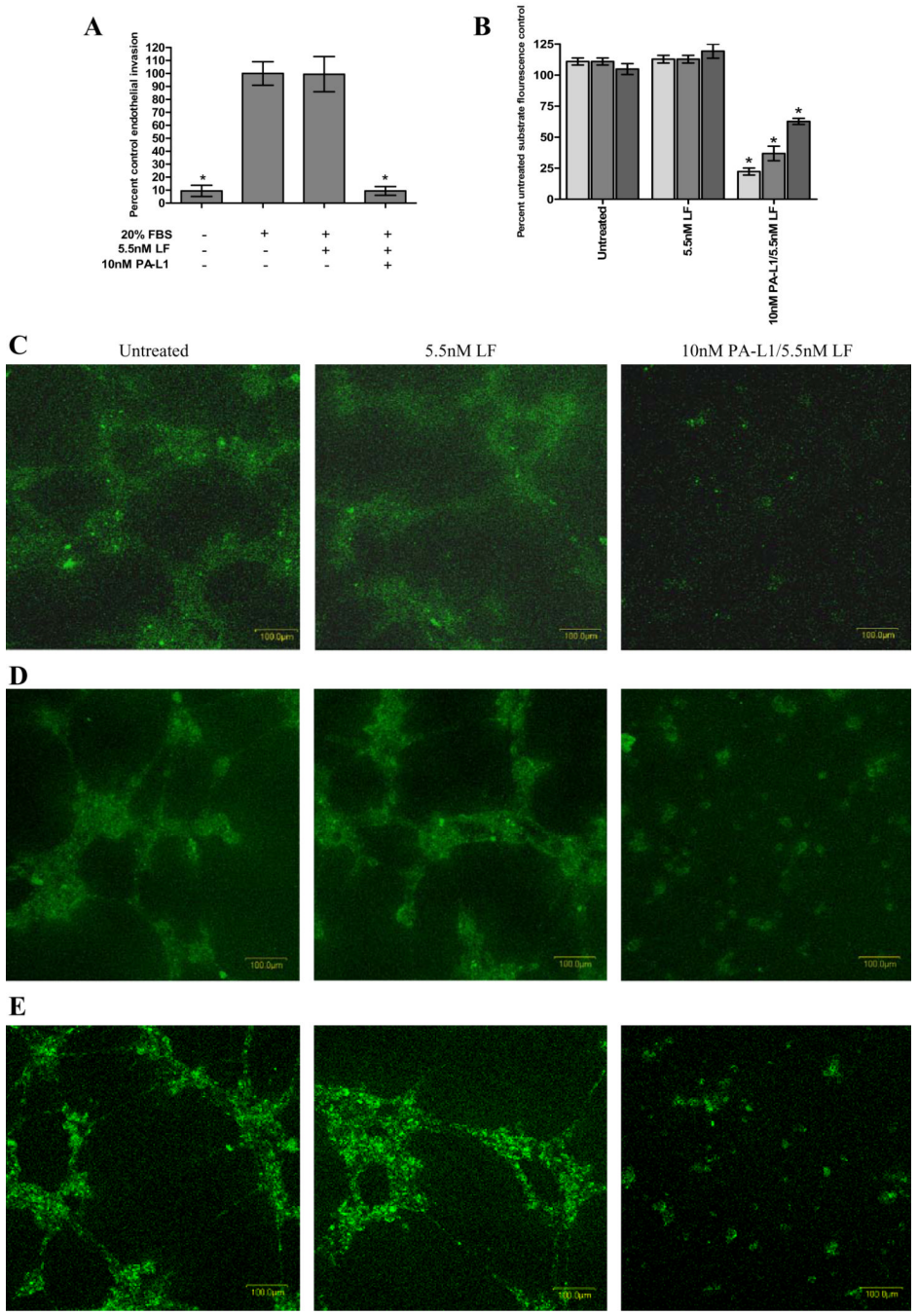

Figure 3.

The extracellular matrix remodeling potential of microvascular endothelial cells is reduced by PA-L1/LF treatment. (A) PA-L1/LF treatment reduced endothelial invasion by >90% ($p<.0001$). In order to dissect these initial observations, PA-L1/LF treated endothelial cell capacity to remodel extracellular matrix was determined. (B) PAL1/LF treated endothelial cells exhibited a significantly reduced ability to cleave collagen type I (75% reduction, light gray bars) collagen type IV (62% reduction, medium gray bars), and gelatin (30% reduction, dark gray bars) ($p<.0001$). Confocal microscopy images (200x total magnification with variable thickness of scans for 15 scans under constant laser intensity and PMT) demonstrating

endothelial cells treated with 10 nM PAL1/5.5 nM LF exhibit a reduced capacity to cleave collagen type I (C) collagen type IV (D) and gelatin (E). * unpaired t test p value <.05.

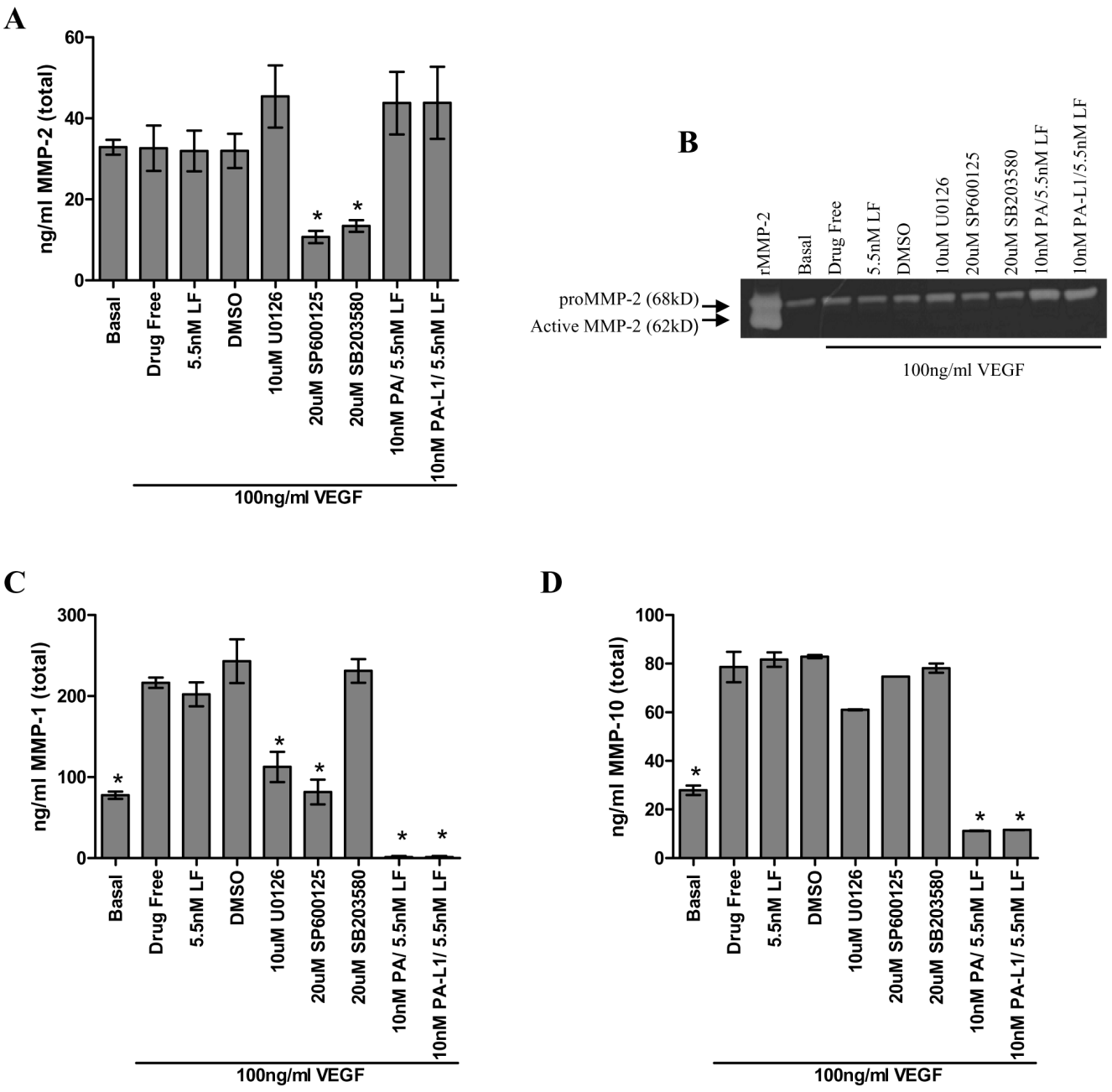

Figure 4.

PA-L1/LF treatment induces the down regulation of proangiogenic endothelial derived MMPs. Microvascular endothelial cells were treated with the toxins/inhibitors, serum starved in the presence of treatments for 16 hours, and then stimulated with complete growth medium supplemented with 100 ng/ml $VEGF_{165}$ in addition to the toxins/inhibitors. Conditioned medium was collected and assayed for proangiogenic MMP expression via ELISA. (A) 10 nM PA and 10 nM PA-L1 in combination with 5.5 nM LF induced an insignificant 34% increase in MMP-2 expression (p = .1482) (B) Cell lysate gelatin zymography demonstrated a 2-fold increase in the localization of MMP-2 on the cell surface in PA and PA-L1/LF treated cells. (C) MMP-1 expression was drastically reduced by >99% in 10 nM PA and 10 nM PA-L1/5.5

nM LF treated endothelial cells (D) MMP-10 expression was not reduced after single MAPK branch inhibition, but reduced by 86% with PA or PA-L1/LF treatment.

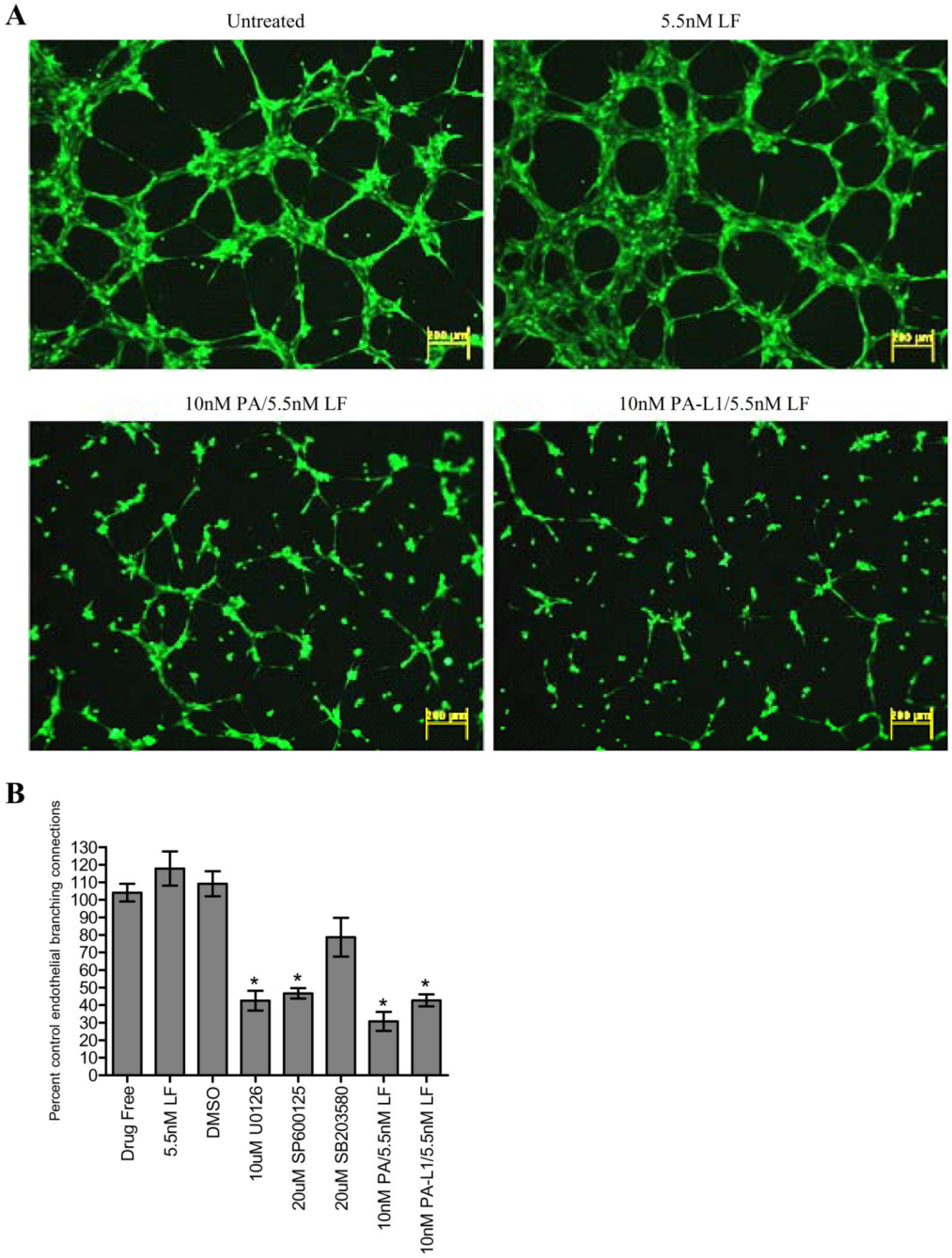

Figure 5.

PA-L1/LF inhibits microvascular endothelial cell tube formation. Endothelial cells were treated with specified concentrations of toxins/inhibitors for 16 hours. Cells were then resuspended in serum free medium in the presence of the treatments and plated on matrigel. Cells were allowed to differentiation into tube structures and either visualized via fluorescent microscopy or analyzed for branching endothelial connections by confocal microscopy. Data is expressed as a percent endothelial branching of the untreated controls. (A) Treatment with 10 nM PA or 10 nM PA-L1 in combination with 5.5 nM LF significantly reduced tube formation by approximately 70 and 60%, respectively ($p<.0001$). Total magnification 40x. (B) U0126-mediated ERK1/2 inhibition as well as JNK inhibition by 20μM SP600125 reduced

tube formation by approximately 60 and 50%, respectively (p<.0001). SB203580 treatment only had modest effects on endothelial cell branching ability (p = .0951). * unpaired t test p value <.05.